Earthquake Engineering. Tenth World Conference © 1992 Balkema, Rotterdam. ISBN 90 5410 060 5

Real time and pseudodynamic tests on a SDoF reinforced concrete structure

E.Gutierrez, G.Magonette, D.Tirelli & G.Verzeletti
Applied Mechanics Division, JRC Ispra, Italy
G.Franchioni
Dynamics Division, ISMES, Bergamo, Italy

ABSTRACT: Experimental data is presented on the dynamic behaviour of a hysteretic SDoF system subjected to a succession of quasi-harmonic inputs. The specimen consists of a full-scale R.C column, having at the free end a large (15 tonnes) pivoted mass. Pseudodynamic (PDT) and Shaking Table (ST) tests were performed, subjecting the column to inertial loading which was designed to cause it considerable damage. We compare the responses obtained from both techniques and examine the motion in terms of hysteretic equivalent damping and natural frequency degradation.

1 TEST SPECIMENS AND SETUP

1.1 Generalities

The experiments were conducted on full-scale, 250x250 mm section, columns of 1.5 m length which are set into an R.C base of 1 m square by 0.5 m deep. The loading configuration represents a column of double the length built in at both ends. The reinforcement consisted of eight 16 mm diameter steel bars and couples of 8 mm stirrups every 50 mm, which conforms to the EUROCODE 8 standard for construction in seismic zones. This specimen type has already been extensively tested in relation to the programme on biaxial bending tests presented in a companion paper (Bousias, 1992). The specimen is seen in Fig. 1 for the ST(a) and PDT (b) test setups.

In the static loading setup, it is possible to carry out biaxial quasistatic bending tests (PDT or otherwise) of up to 140 mm amplitude. A variable compressive load may also be applied through the column axis. The real time dynamic loading setup is the ARIETE shaking table at the ISMES laboratory. The table slides on prismatic bars along one direction and is powered by a 150 kN actuator having a maximum stroke of 200 mm. The maximum payload is 300 kN. The reference signal is sent to the actuator servocontroller directly from an analogue generator.

1.2 Real Time Experimentation

The PDT formulation can, at present, only be realistically applied to lumped parameter systems. In the experiments presented herein,the PDT formulation was that of a SDoF system, consequently the column-mass configuration had to be constructed in such a way as to ensure, that the kinematic idealization in the PDT agreed with the specimen on the shaking table. The main characteristics shown in Fig. 1(a) are as follows: A hinged cross-brace (1) allows the mass to rotate about its axis of gyration Y-Y, but prevents rotation about the normal axis X-X; the mass can translate in the X-X direction which is the kinematic degree of freedom. To prevent rotation of the column about Z-Z (passing through the centre of the column axis), a slender steel plate is fixed to the mass along part of its length (2-3) and is then hinged to a second bracing system at the other end (4). The flexibility afforded by this plate in the Z-Z direction is such that it allows the column to vary in height (as it will do in the plastic regime).

1.3 PDT experiment 1.3 PDT experiment

The PDT configuration shown in Fig. 1(b) is as follows: The kinematic degree of freedom is the direction X-X. Rotation about Z-Z and translation in Y-Y are eliminated by a stiff plate spanning the distance of the reaction frame in the Y-Y direction, but having two nylon rollers (not shown), stiff enough to prevent any significant translation in this direction. The inertial load in a PDT test is modelled analytically, so that in the absence of a real gravity force, the effect of the vertical load on the material properties of the R.C is achieved by applying a constant axial load equal to that of the mass on the dynamic test. However, because the vertical mass load also produces an added moment on the column in proportion to its displacement, an extra term in the al-

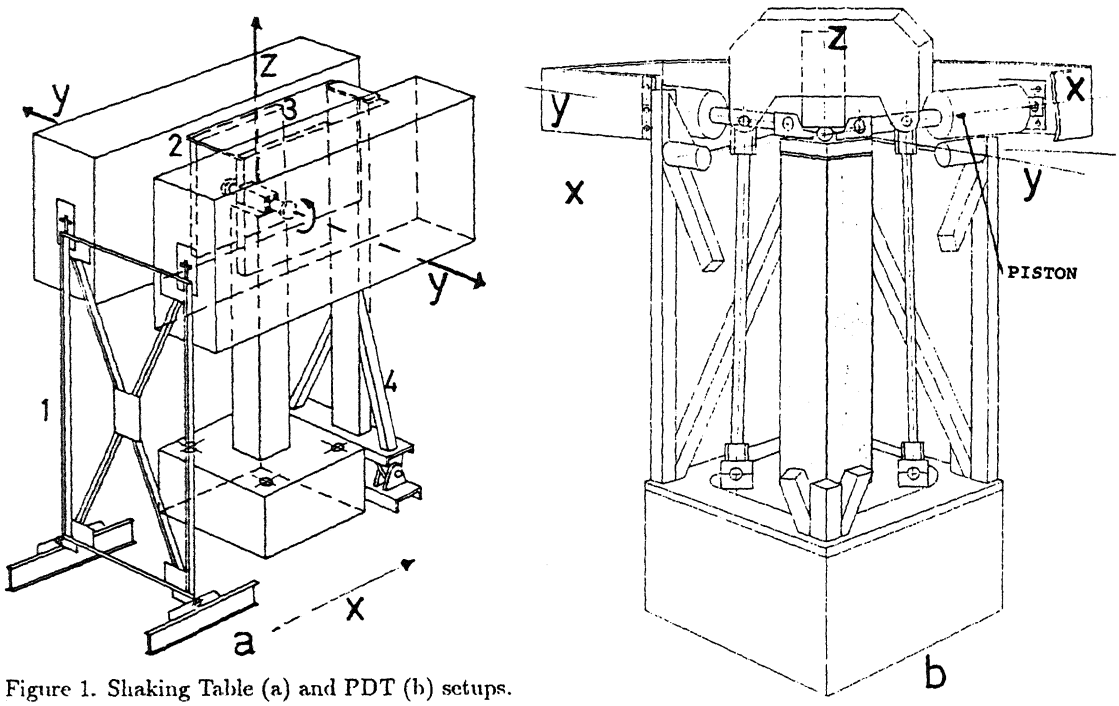

Figure 1. Shaking Table (a) and PDT (b) setups.

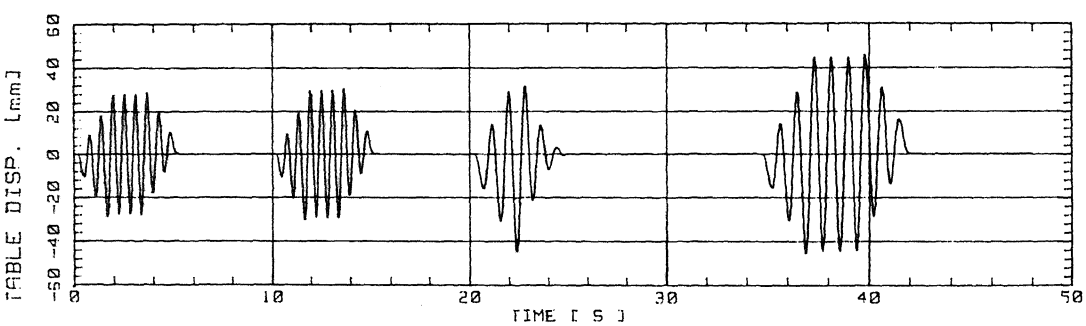

Figure 2. Measured Shaking Table displacement.

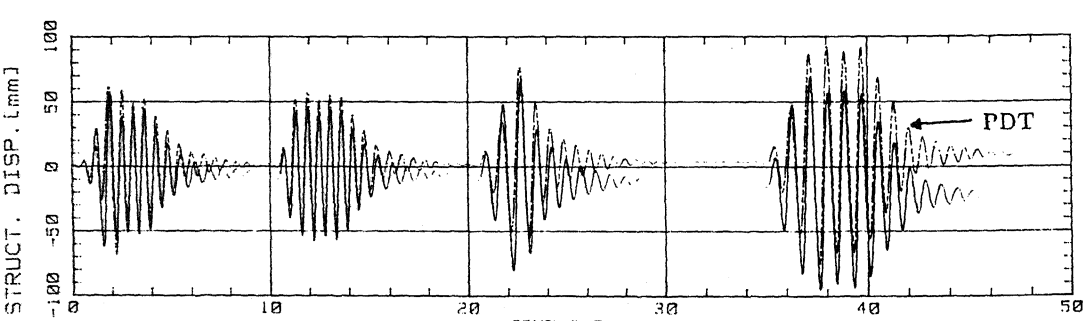

Figure 3. Structural response of Shaking Table and PDT experiments.

gorithm of the equations of motion was included to account for this effect. The constant axial load was provided by an electrohydraulic actuator driven by a classic, analogue PID (Proportional Integral Differential) controller. The actuator controlling the displacement is controlled by a digital loop. In this system the structural displacement is measured by an optical incremental encoder, providing a very accurate measure (Magonette, 1991). The reaction force is the mean of eight recordings measured after a wait period of 0.2s from the end of the previous step; in this way the relaxation effects are reduced to a minimum.

2 INPUT

It consists of an ensemble of amplitude modulated sinusoids. Each of these comprises three segments: two acceleration ramps and a plateau. Each segment lasts for three periods. The analytical expression for the displacement d as a function of time is as follows: for $0 < t < 3T$

$$d = \frac{\alpha}{6\pi}(-2cos\omega t - \omega t sin\omega t + 2)$$

for $3T < t < 6T$

$$d = -\alpha sin\omega t$$

for $6T < t < 9T$

$$d = \frac{\alpha}{6\pi}(-2cos\omega t^* - \omega t^* sin\omega t^* + 2)$$

where

$$t^* = 9T - t$$

The initial conditions are zero for all kinematical variables and derivatives.

3 RESULTS

3.1 Preliminary impact test

Initially, a series of low intensity impact tests were conducted on the specimen with the 15 tonnes mass, from which it was found that the natural frequency was 3.15 Hz. This was somewhat lower than the 3.35 Hz anticipated by the static stiffness measurements (at less than 1 mm displacements) and assumed mass (15000 Kg); the uncertantainties in the boundary conditions of the table-to-base fixtures may be sufficient to account for the discrepancy. The logarithmic decrement index was evaluated as approximately 1.2 % .

3.1 ST test

The data acquisition of the four motions was carried out in four discrete tests. The sampling frequency was modified to accomodate any modulation of the original input signal. Nevertheless , a more than ample total acquisition time was left over to observe the decay of the motion. However, as one of the aims is to compare, vis-a-vis, PDT with ST results we have clipped part of the real-time signal, showing it up to the point where the PDT 'real-time' runs out; to have modelled all the dynamic acquisition in PDT terms would have been unnecessarily long.

3.1.1 Table motion

The basic signal described earlier was repeated four times on the ST. The total input motion is shown in Fig. 3. The target displacement plateaus of each individual envelope are shown in Table 1. The third and fourth motions were intended to have a higher amplitude but a lower frequency than the first two. This modulation was effected because the column had been damaged by the previous motions and its natural frequency had reduced considerably. The initial input-frequency of 1.75 Hz was chosen so as to eventually (on damage) produce a governing frequency ratio of approximately 1.5 in the steady-state part of the motion.

Table 1: Target displacements and frequencies.

Stage no	Amplitude (mm)	frequency (Hz)
1	30	1.75
2	30	1.75
3	45	1.2
4	45	1.2

The first and steady-state table motions had an amplitude of 28 and 30mm, respectively. In motion three, having modulated the input to produce a larger amplitude, the input motion stopped before the plateau. Unfortunately, the table's maximum excursion security limit had not been reset to include the input demanded, consequently, the hydraulic power shutdown was activated. The resulting motion after the peak signal is, paradoxically, a result of the continuing oscillations of the column mass driving the table. Having reset the safety limit, motion number four was performed quite succesfully. The amplitude was 45 mm and the driving frequency was 1.2 Hz as opposed to 1.75.

3.1.2 Response

The term structural displacement as seen in Fig. 3, refers to that measured between the top of the column relative to its base in the X-X direction. During the forcing stages, it is possible to talk of near steady-state (particularly in the second and fourth parts). After the table stops moving, the structural displacement is characterised by a decay history; the analysis will therefore be divided into the steady-

state and decay components.

During the forced motion there are no major beat frequencies. The response is that of a wide band filter; low gain (of the order of 2), and high damping. During the first stage the run-up to the steady-state is not as smooth as in the second. The reason is as follows: given that the initial frequency ratio was 1.75/3.15 (at 1.2 But at the start of the second stage, the natural frequency of the column had degraded approximately by a half (as measured from the decay signal of part one). Given these values the frequency ratio is now approximately 1.75/1.6. The motion of the steady-state in the second stage could well be that of a linear viscously damped system with the appropiate damping and frequency ratios.

Turning now to the decay motions, we must first define it as that motion that occurs after the base input has truly terminated, and not that which appears to be decaying in time. It is hoped that by aligning Figs. 2 and 3 a clearer distinction can be made. The displacement history is analysed on a cycle-per-cycle basis to obtain the natural frequency and damping as functions of time; Figs. 4 and 5. The plots begin after the first few cycles, by which time the driving frequency is dominant and then it is followed by a sudden drop. By this time the structural displacement is that of the column-mass by itself, after which, the natural frequency begins to pick up after 7 seconds and climbs to a value close to the original forcing function. This sequence of events is also seen in the second stage but is not seen in the third or fourth; for these, the trace is nearly monotonically increasing. However, it should be remembered that the forcing function was, by then, 1.2 Hz.

The damping as evaluated from the logarithmic decrement, is shown in Fig. 4, plotted for times just before the input motion has stopped. The initial steep rise in the damping is only apparent because this coincides with the descending branch of the input motion (the periods of input are shown shaded). Later, it is seen to decrease with time and amplitude, albeit slowly, but is not monotonic.It is thought that the oscillations in Fig. 4 are not noise, but actual manifestations of the damping characteristics of the structure. This seems to be backed up by the fact that the corresponding PDT test also produces similar behaviour. In addition, the oscillations have a period of the order of 3-4 seconds, i.e of the order of 8 cycles; this filters out cycle-to-cycle noise when the logarithmic decrement is evaluated.

3.2 PDT EXPERIMENT

We have plotted the results from the PDT test on the same plot as the ST in Fig. 3. During the first stages, the results are in good agreement, but, with time the signals diverge, that is, the plastic offsets increase in opposite directions. However, the comparison of the peak-to-peak displacements, as seen in Fig. 6, is very good. The PDT experiment reproduced very well the dynamic motion in so much as the amplitudes are very similar, but so are the peak excursions. We assume that the specimen is stronger in one direction than in the other due to random variations in material propertie s. Possibly the stronger directions were opposite and this could account for the sign of the offset being different in the two tests.The magnitude of the offset is greater for the dynamic test than the PDT by a factor of 2.

As regards the decaying part of the signals, we have found that the PDT reflects the same tipe of behaviour in terms of cycle-per-cycle frequency and damping properties as in the real-time test. There were some quantitative differences though; the frequency recovery was higher than in the ST test (Fig. 5), but the decay-damping signal was quite similar. Looking back to Fig. 3, it can be seen that the decaying part of the ST is in phase lag to the PDT altough during the forced motion they were in phase. It is thought that these discrepencies are not so much due to any intrinsic difference between PDT and ST testing due to rate-of-loading effect s (Shing and Mahin 1988) (Gutierrez et al 1992), as to the variation in material properties mentioned above.

4 INTERPRETATION OF THE RESPONSE

The motion will be interpreted by describing the nonlinearities in terms of equivalent damping (Jacobsen 1930) and normalised natural frequency. These concepts have been applied in various forms to study the motion of hysteretic systems, but usually they have been aplied to steady-state solutions such as in DebCahudhury (1985) and Jennings (1968) where the equivalent parameters have been taken as single-valued functions of the displacement for single-frequency input content. In reality the displacement signal is rarely monocromatic and the equivalent parameter properties are far from being single-valued functions of the displacement. A paper which addresses this last point from an experimental aspect is that of Iemura and Jennings (1974).

For R.C structures it is difficult to assess the variation of these properties as functions of the displacement history.In Fig. 7 the hysteresis loops of the PDT test have been plotted for the first stage of the motion. From these loops it is possible to evaluate the equivalent damping as a function of the displacement amplitude (the offset is not considered). Also the 'normalised frequency degradation' (f') can be evaluated as a function of displacement amplitude by dividing the frequency obtained from the secant stiffness by the undamaged measured frequency (as in the case of the dynamic test above, or obtained from the static, low-level amplitude, undamaged stiffness for the PDT). By cro splotting the equivalent damping with f', Fig. 8 is obtained (parameter plane) from the loops of Fig. 7. As a guide some of the key features of the first stage of the structural motion have been identified on the parameter plane. The region of near steady-state motion (Fig. 3 be-

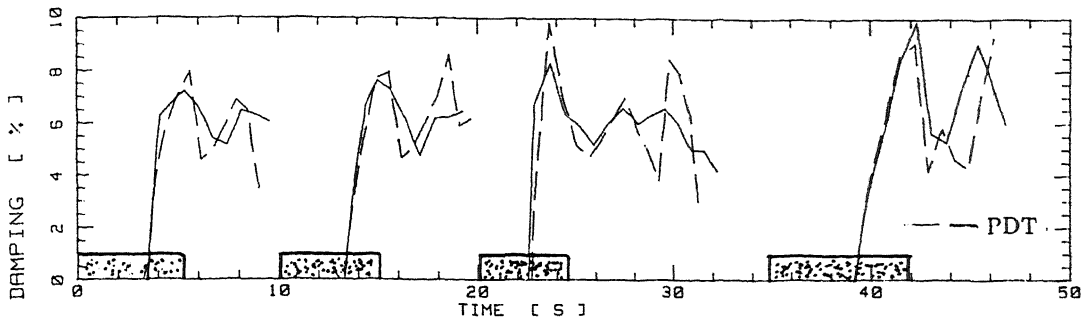

Figure 4. Damping evaluated from logarithmic decrement. The periods of the forcing function are showm (hatched) to indicated the onset of natural decay.

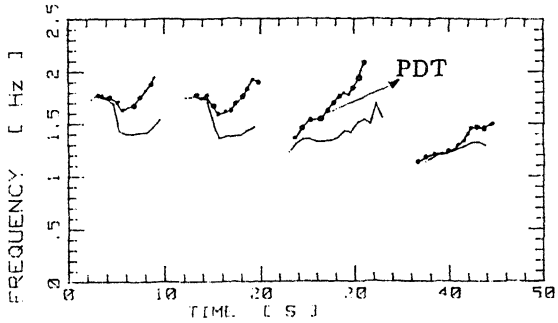

Figure 5. Variation of response zero-crossing frequency

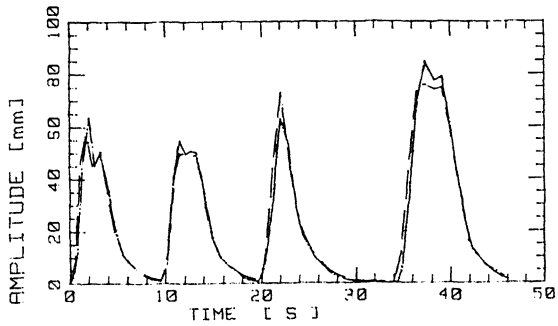

Figure 6. Comparison of mean amplitude of oscillation for ST (continuous line) and PDT experiments.

gins to appear at about 3 seconds, the normalised frequency, from Fig. 8, is .45 (1.5 Hz) of the undamaged frequency (3.23 Hz); thus the governing frequency ratio was 1.4; in addition, we have that the equivalent damping, from Fig. 8, is 18 % (for the fourth stage the value is as high as 25%). Given such values, the resonance curve under steady-state conditions would result in a gain of 1.8. As shown on Fig. 2, the base input amplitude at this stage was 28 mm, thus the structural amplitude should be 50.4 mm, this value agrees quite well with the average peak-to-peak displacement amplitude of Fig. 6.

During the decaying motion, as indicated in Fig. 8, the reduction of the amplitude brings about an increase in the natural frequency of the structure, while at the same time the damping is reduced from 18 % to about 8-10. In Fig. 5 a drop in the frequency is first observed when the input motion stops; the reason being that the structural natural frequency by itself is incompatible with the displacement amplitude at that stage (if it is assumed that the secant stiffness governs the period of oscillation), and so the frequency will accomodate to these conditions, i.e it slows down. After 6 seconds the natural frequency picks up again, this is because the amplitude continues to decay, and with decreasing amplitude the secant stiffness (consequently f') will increase.

At the onset of the decaying oscillations in the second and fourth motions, the forcing function had been 1.2 Hz. Although the oscillations start off from higher displacement amplitudes than the first two stages, the compatibilty of the natural and input frequencies at that amplitude is greater. For this reason the frequency recovery curve does not show the discontinuity observed in the first stages. In Fig. 4 we have shown that during the decaying amplitude, the logarithmic decrement damping decreased nonmonotonically while the natural frequency increased continuously. This phenomenon is observed in the paramcter plane (Fig. 8) as a curling of the damping after point 4. Thus, the frequency and damping properties obtained from the displacement versus time measurements are correlated in the parameter plane as obtained from the force displacement loops.

5 CONCLUSION

PDT and ST tests have been conducted on a full-scale R.C column-mass system. The input produced

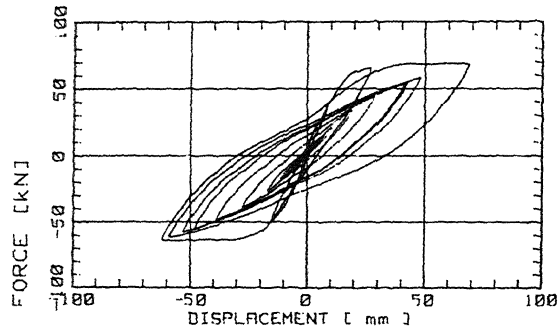

Figure 7. Hysteresis loops for first stage of PDT test (gravity loading moment is included).

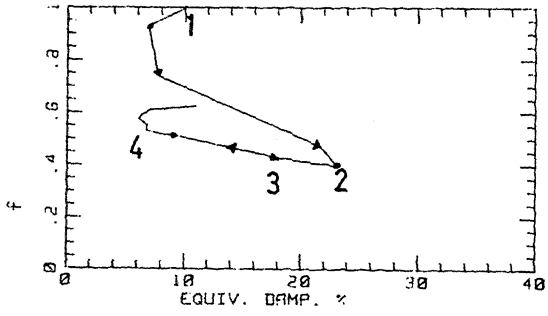

Figure 8. Normalised frequency versus equivalent damping as evaluated from hysteresis loops. 1->2 Transient start-up. 3 Steady-state region. 4-> Decaying phase.

a large hysteretic response. The comparison of the PDT and ST techniques was quite successfull in terms of the structural displacement. The PDT method offers the advantage of registering the restoring forces directly and clearly, from which clean hysteresis loops are obtainable for further analysis. By viewing the motion in terms of equivalent damping and normalised natural frequency it is possible to better understand the motion. It has been shown that ductile R.C columns behave as variable low gain (up to the order of 2), high damping filters (up to 25 % in near steady state conditions). The filter properties are non-stationary and depend on the amplitude of the displacement and displacement history. A model that defines these properties in terms of the displacement history and how it may be used in a dynamic non-linear analysis is at present being prepared.

ACKNOLEDGEMENTS

The authors would like to thank P. Negro for his help in the definition of the input and Messrs Tognoli and Tamborini for the mecanical design of the specimen fixtures.

REFERENCES

Bousias, S.N., Verzeletti, G., Fardis, M.N, Magonette, G., "RC Columns in biaxial bending and axial load" *submitted to the 10th World* Conf. in Earthq. Eng. Madrid, 1992.

DebChaudhury, A. "Periodic Response of Yielding Oscillators" J. Engrg. Mechs. Div., ASCE, vol. 111, No. 8, 1985, pp 977-994.

Gutierrez, E., Magonette, G., Verzeletti, G. "Rate of Loading Rate Effects on the Cyclic Response of R.C Columns" accepted for publication in J. Engrg. Mechs. Div., ASCE, 1992.

Iemura, H. and Jennings, P.C. "Hysteretic Response of a Nine-Storey R.C Building", Earthq. Engrg. Struct. Dyn., vol.3, 1974, pp 183-201.

Jacobsen, L. S. "Steady Forced Vibration as Influenced by Damping",Trans. ASME, vol 52, part 1, 1930, pp 169-181.

Jennings, P. C. "Equivalent Viscous Damping for Yielding Structures", J. Engrg. Mechs. Div., ASCE, vol. 94, No.EM1, 1968, pp 103-116.

Magonette, G. "Digital Control of Pseudodynamic Tests ", Experimental and Numerical Methods in Earthquake Engineering, ed. Donea J. and Jones P, Kluwer Academic Press, 1991,pp 63-99

Shing, P., and Mahin, A., "Rate-of-Loading Effects on PseudodynamicTests", J. Struct. Div., ASCE, vol. 114,. No 11, 1988, pp 2403-2420.